



HHS Public Access

Author manuscript

Eur J Pharm Biopharm. Author manuscript; available in PMC 2016 May 01.

Published in final edited form as:

Eur J Pharm Biopharm. 2015 May ; 92: 74–82. doi:10.1016/j.ejpb.2015.02.006.

Evaluation of Topical Hesperetin Matrix film for Back-of-the-Eye Delivery

Goutham R. Adelli¹, Tushar Hingorani¹, Nagendra Punyamurthula¹, Sai Prachetan Balguri¹, and Soumyajit Majumdar^{1,2,3,#}

¹Department of Pharmaceutics and Drug Delivery, School of Pharmacy, The University of Mississippi, University, Mississippi 38677

²Research Institute of Pharmaceutical Sciences, The University of Mississippi, University, Mississippi 38677

³National Center for Natural Product Research, The University of Mississippi, University, Mississippi 38677

Abstract

Purpose—The goal of the present study is to develop a poly (ethylene oxide) N10 (PEO N10) based melt-cast matrix system for efficient and prolonged delivery of hesperetin (HT), a promising bioflavonoid, to the posterior segment of the eye through the topical route.

Methods—HT film was prepared by melt-cast method using PEO N10 and cut into 4 mm × 2 mm segments, each weighing 8 mg. This film was evaluated with respect to *in vitro* release rates and also transmembrane delivery across Spectra/Por[®] membrane (MWCO: 10000 Daltons) and isolated rabbit corneas. Ocular tissue concentrations were also determined post application of the film in *ex vivo* and *in vivo* models.

Results—HT release from the film was determined to be about 95.3 % within 2 h. *In vitro* transcorneal flux was observed to be $0.58 \pm 0.05 \mu\text{g}/\text{min}/\text{cm}^2$ across the isolated rabbit cornea. High levels of HT were detected in the retina-choroid (RC) and vitreous humor (VH) in the *ex vivo* model following topical application of the film. Significant levels of HT were observed in both anterior and posterior segment ocular tissues 1h post topical application of the 10 and 20 % w/w HT films on the rabbit eye. Moreover, HT was detected in the VH and RC even after 6h following topical application of the film *in vivo*.

Conclusion—The results from this study suggest that the melt-cast films can serve as a viable platform for sustained topical delivery of bioflavonoids, and other therapeutic agents, into the back-of-the eye tissues.

© 2015 Published by Elsevier B.V.

#Author for correspondence: Soumyajit Majumdar, 111 Faser Hall, Department of Pharmaceutics and Drug Delivery, School of Pharmacy, The University of Mississippi, University, MS 38677; Tel: (662)-915 3793; Fax: (662)-915-1177; majumso@olemiss.edu.

Publisher's Disclaimer: This is a PDF file of an unedited manuscript that has been accepted for publication. As a service to our customers we are providing this early version of the manuscript. The manuscript will undergo copyediting, typesetting, and review of the resulting proof before it is published in its final citable form. Please note that during the production process errors may be discovered which could affect the content, and all legal disclaimers that apply to the journal pertain.

Keywords

Hesperetin; bioflavonoids; hot melt extrusion; melt-cast technology; polyethylene oxide; polymeric matrix film; topical application; sustained delivery; back-of-the eye delivery

1. Introduction

Diseases affecting the posterior segment of the eye such as diabetic retinopathy (DR), age related macular degeneration (AMD), diabetic macular edema (DME) and proliferative vitreo-retinopathy (PVR) are some of the major causes of blindness in the United States [1-3]. According to the World Health Organization (WHO) approximately 39 million people are affected by vision loss and 246 million people suffer from moderate to severe vision impairment. Based on the 2010 U.S census, out of the 142.6 million above 40 years of age, 7.6 million people suffer from DR and 2.1 million are affected by AMD.

In case of DR, hyperglycemia and tissue hypoxia causes thickening of the capillary basement membrane and death of pericytes. Damage to the pericytes causes microaneurysms, vascular leakage and blockage of retinal capillaries leading to oxidative stress. High amounts of polyunsaturated fatty acids (primary targets of peroxidation), generation of free radicals through frequent photoexcitation and adequate oxygen supply are the three major causes of oxidative damage to the retina. Many studies have also reported the relationship between high blood glucose and oxidative stress and initiation of DR [4-7].

In early stages of AMD, accumulation of drusen (sub-RPE deposits) under the retinal pigmented epithelium (RPE) affects the macula and leads to the loss of central vision. This is followed by choroidal neovascularization (CNV) in the subretinal spaces. Progressive accumulation of abnormal chemicals in Bruch's membrane and formation of drusen aggregates lead to neovascular leakage and degeneration of the RPE cells [8].

Bioflavonoids, a group of plant polyphenols, are reported to exhibit antioxidant, anti-angiogenic and anti-inflammatory properties along with fluid retention reduction and capillary wall strengthening activities [9, 10]. Hesperidin (HD), and its aglycone hesperetin (HT), a plant based flavanone (Figure. IA & B) obtained from *Citrus sinensis*, possess antioxidant [11, 12], and neuroprotectant properties [11], and reduces vascular permeability. HT is recognized to be more potent than HD in scavenging reactive oxidative species (ROS) [13-15]. HT also prevents the cytotoxic effect of peroxynitrites by converting them to non-toxic mono-nitrated products and increasing phosphorylation of extracellular-signal-regulated kinases (ERKs) [16]. Anti-inflammatory activity of HT is thought to be achieved by inhibition of the COX-2 pathway and synthesis of PGE₂ [17], and inhibition of nitric oxide production by blocking nitric oxide synthase [18, 19]. Additionally, HT was observed to increase ocular blood flow and promote recovery of retinal function following ischemic insult of retina [20]. Currently HT is available as an oral dietary supplement to improve blood flow and as a vasoprotectant. Cumulative urinary recovery of HT suggests a bioavailability of less than 25 % after oral administration of HD and HT [21]. Poor oral bioavailability of HT can be attributed to its rapid metabolism into hydrophilic glucuronide

metabolites [22] and short half-life (Plasma half-life: 6.7 h and vitreous humor half-life: 110 min) [23, 24].

Treating the posterior segment eye diseases has always been a great challenge because of the unique physiological and anatomical barriers of the eye. Our earlier studies demonstrate that systemic application fails to deliver HT to the ocular tissues [22]. This makes topical or intraocular/periocular application the most effective. Less than 5 -10 % of topically applied drug, however, permeates into the intraocular tissues [25-27]. Various ocular delivery systems are being investigated to increase drug contact time and site specific delivery to the posterior segment of the eye using liposomal formulations and other sustained release and controlled release systems such as ocular inserts, collagen shields, matrix systems, and hydrogel lenses [28-31].

The goal of the present study is to evaluate the effectiveness of topical melt-cast polymeric matrix systems with respect to the delivery of HT to the back-of-the-eye tissues, especially to the retina-choroid (RC) and vitreous humor (VH). The matrix film was evaluated *in vivo* for dose dependent and time dependent drug delivery.

2. Materials and methods

2.1. Chemicals

PEO (PubChem CID: 5327147) [PolyOx[®] WSR N-10 (PEO N-10), MW: 100,000 Daltons] was kindly donated by Dow Chemical Company (Midland, MI). HT (PubChem CID: 72281) (Type HP-2, from *Helix pomatia*) was purchased from Sigma Aldrich (St. Louis, MO). All other chemicals were purchased from Fisher Scientific (St. Louis, MO).

2.2. Animal tissues

Whole eye globes of New Zealand albino rabbits were purchased from Pel-Freez Biologicals[®] (Rogers, AK), shipped overnight in Hanks Balanced Salt Solution (HBSS) over wet ice [32]. Corneas and whole eye globes were used on the day of receipt.

2.3. Animals

Male New Zealand albino rabbits (2.0 - 2.5 Kg) procured from Harlan Laboratories[®] (Indianapolis, IN) were used in all the studies. All animal experiments conformed to the tenets of the Association for Research in Vision and Ophthalmology statement on the Use of Animals in Ophthalmic and Vision Research and followed the University of Mississippi Institutional Animal Care and Use committee approved protocols.

2.4. Preparation of polymeric matrix film

Melt-cast method was employed in the preparation of the polymeric matrix film. PEO N10 (Figure 1C) was selected as the matrix forming polymer. A physical mixture of HT and PEO N10 was prepared by geometric dilution. Drug load in the film was 10 % or 20 % of the total weight of film. A 13 mm die was placed over a brass plate and heated to 70 °C using a hot plate. The physical mixture of HT and polymer was added in the center of the die and compressed to form a flat matrix surface. The mixture was further heated for 2-3 min. After

cooling, 4 mm × 2 mm sections each weighing approximately 8 mg and with a drug load of 0.8 mg or 1.6 mg for the 10 %w/w and 20 %w/w films, respectively, were cut out from the film.

2.5. Assay and content uniformity

To determine HT content, the film was placed in a mixture of methanol and dimethyl sulfoxide (DMSO) 50:50 and sonicated for 15 min until the film was completely dissolved in the solvent mixture. Content uniformity was determined using four separate sections of 8 mg each, randomly cut from a single 13 mm film, and analyzed as described under analytical procedure using an HPLC-UV method.

2.6. Differential scanning calorimetry (DSC) and Fourier transform infrared spectroscopy (FTIR)

DSC thermograms for pure HT, PEO N10 and the 10 %w/w film was collected using a Diamond Differential Scanning Calorimeter (Perkin-Elmer[®] Life and Analytical Sciences) [33]. The samples were weighed and sealed in aluminum pans and were heated from 0 °C to 270 °C at a heating rate of 10 °C/min under nitrogen purge (20 mL/min). Infrared spectra (IR) for PEO N10, HT, and melt-cast film (10 %w/w and 20 %w/w) were obtained using a Cary 660 series FTIR (Agilent Technologies) and MIRacle™ Single Reflection ATR (PIKE Technologies). Further, the IR spectrum of the 13 mm matrix film was collected randomly from different areas of the film, to evaluate distribution uniformity within the polymer matrix.

2.7. *In vitro* release and corneal permeability studies

To study the release profile of HT from the film, *in vitro* release studies were carried out as depicted in figure II. Three 20 mL glass vials were taken and a 10 %w/w film (8 mg; Dose: 0.8 mg) was placed at the bottom of each vial. A standard US 100 mesh sieve was placed over the film and a magnetic bead was placed on the sieve. The glass vials were placed over a magnetic stirrer. Similar set up was employed in 3 more vials but without the sieve and the magnetic stirrer to evaluate the barrier characteristics of the sieve, if any. In both cases, 18 mL of 5 %w/v HPβCD was used as the release/dissolution medium to ensure sink conditions were maintained (0.6 mg of HT is soluble in 1 mL of 5 %w/v HPβCD). The temperature was maintained at 34 ± 2 °C using hot plates. Aliquots, 0.8 mL, were collected at specific time intervals and replaced with an equal volume of release medium. The release studies were carried out for a period of 2 h. Samples were analyzed using a HPLC-UV method.

In vitro corneal permeability of HT from the matrix film was evaluated using a side-by-side diffusion apparatus (PermeGear, Inc., Hellertown, PA) for 3 h (Fig. III). The studies were carried out by sandwiching the film (4 mm × 2 mm; 10 %w/w HT; weighing 8 mg approximately; 0.8 mg HT) in between a Spectra/Por[®] membrane (MWCO: 10,000 Daltons) and isolated rabbit cornea (Pel-Freez Biologicals; Rogers, AK). Corneas were excised from whole eye globes, following previously published protocols [32], with approximately 1 mm scleral portions remaining for ease of mounting. The membrane-film-cornea sandwich was then placed in between the side-by-side diffusion cells (the chamber towards the Spectra/Por[®] membrane representing the periorcular surface and the chamber towards the cornea

representing the aqueous humor) and samples were collected and analyzed as described above under release study. The side-by-side diffusion cells maintained at 34 °C using a circulating water bath. Five percent HP β CD in isotonic phosphate buffer saline (IPBS) (pH 7.4) was used as the receiver medium. Aliquots (0.6 mL) were drawn at every 30 min interval and replaced with an equal volume of fresh buffer. Samples were analyzed by a HPLC-UV method.

2.8. *Ex vivo* studies

Whole eye globes obtained from Pel-Freez were placed in 12 well tissue culture plates containing IPBS (pH 7.4) with corneas facing upwards. IPBS was added to the wells and was maintained below the level of corneo-scleral-limbus. The whole set up was maintained at 34 °C using a water bath. The 10 % w/w HT film was placed at the corneo-scleral-limbus and the eye globes were allowed to stand for 3 h. At the end of 3 h the surface of the eye globes were washed thoroughly and aqueous humor (AH), vitreous humor (VH) and retina-choroid (RC) were carefully isolated and analyzed for HT content.

2.9. *In vivo* bioavailability studies

Male New Zealand albino rabbits weighing between 2.0 - 2.5 Kg were used to determine *in vivo* bioavailability of HT from the matrix film in a time and dose dependent manner. Rabbits were anesthetized, using a combination of ketamine (35 mg/kg) and xylazine (3.5 mg/kg) injected intramuscularly, and maintained under anesthesia throughout the experiment. In these studies, either the 10 % or the 20 % w/w HT loaded films were placed in the conjunctival sacs of the rabbit eye. At the end of 1h and 3h (for both doses) and 6h (for the 20 % w/w film) after topical application, the rabbits were euthanized under deep anesthesia with an overdose of pentobarbital injected through the marginal ear vein. The eyes were washed with ice cold IPBS and immediately enucleated and washed again. Ocular tissues were separated, weighed and preserved at -80 °C until further analysis. All experiments were carried out in triplicate.

2.10. Corneal histology

Corneas exposed to the 20 % w/w HT film (highest dose tested) for 6h (longest duration) *in vivo* were collected and evaluated for histological characteristics. Corneas excised from the contralateral eyes were used as controls. Extracted corneas were fixed in 2 % w/v paraformaldehyde and 2 % v/v gluteraldehyde in IPBS. Histological evaluation was carried out at Excalibur Pathology Inc. (Oklahoma City, OK) as per previously reported protocols [34]. Corneas embedded in paraffin were sliced into 5 μ m cross sections using a microtome (American Optical® 820 Rotary Microtome). These sections were placed on a slide and dried overnight in an oven at 68 °C. The slide was washed with xylene to remove paraffin and washed with alcohol and water to hydrate the tissue. This was then stained with nuclear dye Gill III hematoxylin (StatLab medical) for 10 min and rinsed, and then counterstained with eosin. These slides were then washed in reverse manner (running water, alcohol, and xylene), cover slipped and examined under microscope (Chromavision ACIS II).

2.11. Analytical procedure for *in vitro* Samples

Waters HPLC system with 600 E pump controller, 717 plus auto sampler and 2487 UV detector was used. Data handling was carried out using an Agilent 3395 integrator. HT stock solution was prepared in acetonitrile (ACN). A 50:50 mixture of 20 mM phosphate buffer (pH 2.5) and ACN was used as mobile phase with Phenomenex Luna[®] 5 μ m C₁₈ 100 Å, 250 \times 4.6 mm column at a flow rate of 1 mL/min and 284 nm.

2.12. Bio-analytical method

2.12.1. Standard solution preparation—To 100 μ L of aqueous humor (AH) or 500 μ L of vitreous humor (VH) and to a weighed amount of the cornea, sclera, iris ciliary bodies (IC) and retina-choroid (RC), 20 μ L of HT stock solution in ACN (0.5, 1, 2.5, 5, 7.5, and 10 μ g/mL) was added and allowed to stand for 5 min. To precipitate the proteins, ice cold ACN was added to the AH and VH standards in 1:1 ratio and 1 mL to the cornea, sclera, IC and RC standards. Final concentrations of the standard solutions prepared were in the range of 10 - 200 ng/mL for AH; 10 - 100 ng/mL for VH; 20 - 200 ng/mL: cornea & sclera and 10 - 200 ng/mL: IC & RC. All samples were centrifuged at 13,000 rpm and 4 °C for 30 min and analyzed using HPLC-UV. All the standard curves generated an R² value greater than 0.95. Average recovery values were determined in AH (93.5 %), VH (94.7 %), IC (92.1 %), RC (97.3 %), cornea (89.6 %) and sclera (88.7 %).

2.12.2. Sample preparation—Approximately 0.1 mL of AH and 0.5 mL of VH was collected from each test eye into individual centrifugal tubes. All other tissues, RC, IC, cornea & sclera, from each test eye were individually cut into very small pieces and placed into individual vials. Protein precipitation was carried out similar to the standard solution preparation and analyzed using HPLC-UV method.

A mixture of 20 mM phosphate buffer (pH 2.5) and ACN in a ratio of 65:35 was used as the mobile phase and Phenomenex Luna[®] 5 μ m C₁₈ 100 Å, 250 \times 4.6 mm column at a flow rate of 1 mL/min and 284 nm.

2.13. Data analysis

All experiments were carried out at least in triplicate. HT release data was fitted to zero order, first order and Higuchi models (Equations 1, 2 & 3).

$$C_t = C_0 + K_0 t \quad \text{Eq (1)}$$

$$\text{Log} C_t = \text{Log} C_0 + K t / 2.303 \quad \text{Eq (2)}$$

$$C_t = K_H t^{1/2} \quad \text{Eq (3)}$$

Where,

C₀ & C_t = concentration at time 0 min and t min,

K_0 , K & K_H = kinetic constants for zero order, first order and Higuchi models.

Drug diffusion parameters across cornea such as cumulative amount (M_n), rate (R) and flux (J) were calculated using previously described method [35].

Cumulative amount of HT released from the film was calculated using equation 4

$$M_n = V_r C_{r(n)} + \sum_{X=1}^{X=n} V_{s(X-1)} C_{r(X-1)} \quad \text{Eq (4)}$$

Where,

n = sampling time point ($n=1, 2, 3$ and $4 \dots$ corresponding to 15, 30, 45 and 60.. min respectively),

V_r = volume of the medium in the receiver chamber (mL),

V_s = volume of the sample withdrawn at the n^{th} time point (mL),

$C_{r(n)}$ = concentration of the drug in the receiver chamber medium at n^{th} time point ($\mu\text{g/mL}$).

Steady state flux was determined using equation 5

$$\text{Flux}(J) = \frac{(dM/dt)}{A} \quad \text{Eq (5)}$$

Where,

M = cumulative amount of HT (μg),

t = time (min),

A = surface area of cornea (0.636 cm^2).

Statistical analysis was carried out using ANOVA to compare between different groups and Tukey's post-hoc HSD was used to compare differences between two groups. A 'p' value less than 0.05 was considered to denote statistically significant difference.

3. Results

3.1. Assay and content uniformity studies

HT content in all the films was observed to be approximately between 90 – 93 % of the theoretical values and was found to be uniformly distributed within the matrix (RSD < 2.3 %).

3.2. DSC and FTIR studies

DSC thermograms of pure PEO N10, pure drug and polymeric film are presented in Figure IV. HT exhibited an endotherm at 234 °C corresponding to its melting point. PEO N10

exhibited a melting point temperature of 65 °C. PEO N10 demonstrated an endothermic peak shift from 65 to 63 and 60 °C with the 10 %w/w and 20 %w/w films, respectively. HT peak at 245 °C was absent in the melt-cast films.

FTIR spectra of pure HT showed aromatic stretching from 1650 to 1500 cm^{-1} , and –OH phenolic stretching was observed at 1200 cm^{-1} . Pure PEO revealed –CH stretching at 2890 cm^{-1} . Scissoring and wagging movement of –CH₂ were observed at 1450 and 1350 cm^{-1} . Aromatic stretch bands corresponding to HT and –CH stretch bands corresponding to PEO N10 were observed with the 10 %w/w film. Similar spectral bands were observed with the 20 %w/w film (Figure VA & B).

3.3. *In vitro* release and corneal permeability studies

Release of HT from the matrix films was 95.3 ± 1.3 % (with sieve) and 89.3 ± 11.9 (without sieve and no stirring) within 120 minutes (Figure VI).

Rate and flux across the corneal and Spectra/Por[®] membranes were found to be 0.37 ± 0.03 $\mu\text{g}/\text{min}$ and 0.58 ± 0.05 $\mu\text{g}/\text{min}/\text{cm}^2$ and 0.57 ± 0.05 $\mu\text{g}/\text{min}$ and 0.89 ± 0.06 $\mu\text{g}/\text{min}/\text{cm}^2$, respectively (Figure VII). Under the settings employed release towards the periocular surface (representing the precorneal loss) of HT from the film was found to be 16.1 ± 4.5 % in 3 h. Cumulative precorneal loss of HT was 1.7-folds higher than that observed across the cornea. Cumulative amount of HT permeating across the isolated rabbit cornea in 3 h was determined to be 59.9 ± 5.2 μg .

3.4. *Ex vivo* studies

HT content in the AH, VH and RC were found to be 5.8 ± 0.2 $\mu\text{g}/\text{gm}$ of tissue, 5.6 ± 1.4 $\mu\text{g}/\text{gm}$ of tissue, and 14.2 ± 3.8 $\mu\text{g}/\text{gm}$ of tissue, respectively. Amount of HT in RC was found to be 2.5-fold higher compared to that in the AH or VH.

3.5. *In vivo* studies

Initially, ocular tissue concentrations obtained with 10 %w/w HT loaded matrix film was evaluated *in vivo* 1h after topical application of the film. AH, VH, IC, RC, cornea and sclera were analyzed for HT content. Significant levels of HT were detected in the IC, cornea and sclera tissues. HT levels were also observed in the back-of-the-eye tissues: VH (0.05 ± 0.03 $\mu\text{g}/\text{gm}$ of tissue) and RC (7.8 ± 0.2 $\mu\text{g}/\text{gm}$ of tissue). When, HT load in the film was doubled (Dose: 1.6 mg per 4 mm \times 2 mm; 8 mg of film) HT levels in the AH, IC, and cornea were 2-fold higher than that of the 10 %w/w HT film. With the 20 %w/w film, amount of HT in the posterior segment ocular tissues was found to be 1.4 ± 0.5 $\mu\text{g}/\text{gm}$ of tissue (VH) and 23.5 ± 6.9 $\mu\text{g}/\text{gm}$ of tissue (RC). It was observed that doubling the dose of HT in the matrix resulted in an approximately 10- and 28-fold increase in scleral and VH HT concentrations, respectively. The results are presented in Figure VIII A&B; Table I.

Ocular tissue concentrations, 3 h post topical instillation of the 10 %w/w and the 20 %w/w HT film *in vivo*, were also evaluated. Expectedly, HT concentrations at the end of 3h were relatively low compared to the 1 h time point. Results from the 3 h study are presented in Figure VIIIA&B; Table I.

Ocular tissue HT concentrations obtained with the 20 % w/w film was tested 6 h post topical application. HT was detected in VH (0.03 ± 0.02 $\mu\text{g}/\text{gm}$ of tissue), RC (0.4 ± 0.02 $\mu\text{g}/\text{gm}$ of tissue), IC (1.5 ± 0.1 $\mu\text{g}/\text{gm}$ of tissue) and sclera (6.1 ± 1.6 $\mu\text{g}/\text{gm}$ of tissue) (Figure VIII B & Table I). Only the posterior segment ocular tissue concentrations were determined in the 6h study as the cornea was carefully isolated and taken for histology studies. Thus, both cornea and AH HT concentrations were not determined in the 6h study.

3.6. Corneal histology

Corneas exposed to the 20 % w/w HT film for 6 h did not show any substantial damage when compared to the control. Extracellular swelling of the corneal epithelium or stromal lamellae was observed in the control and the corneas exposed to the film representing the minor artifacts that were introduced during the fixating process (Fig. IX).

4. Discussion

In this study HT was incorporated into a polymeric matrix system utilizing a melt-cast method. In this method, the active compound is embedded in a carrier matrix comprised of one or more meltable substances and other functional excipients. Once the formulation comes into contact with the release media (*in vitro*) or tear fluid (*in vivo*) it quickly transforms into a gel and releases the drug slowly over prolonged periods of time, depending on the matrix composition. Moreover, high drug loads (20 - 40 % w/w) can be easily incorporated without the need for any organic solvent. Importantly, both hydrophilic and hydrophobic moieties can be incorporated into the polymeric matrix without any difficulty. Considering the low volumes that can be administered topically (35 - 50 μL in general) and the fact that a large number of new drug candidates are poorly water soluble, most of the current dosage forms require surfactants or other solubilization approaches. The melt-cast technology converts the compounds into its amorphous state, or disperses them at a molecular level in the polymer matrix, because of which the solubility of the compound is increased. Increased solubility could improve transcorneal permeability of the therapeutic agent several folds. By altering the type of matrix polymer, this process technology can be employed to design sustained release dosage forms.

The calculated pKa of HT, obtained using ACD/I-Lab Web Service (ACD/log P 8.02 and ACD/pKa 8.03), is 7.9; this results in increased permeability in the neutral and slightly acidic pH range [36]. The tear pH can range between 6.5-7.6 [37, 38]. Thus, transcorneal permeability of HT could be influenced by the tear pH to some extent as the percentage HT in the unionized form could vary from about 66% to 96% depending on the tear pH. The pH of the melt-cast films prepared in this study was observed to be 7.0 in the gel state, a pH at which about 90% of the HT remains in the unionized state favoring greater permeability across the ocular tissues. Besides ionization state, however, a host of other formulation, physicochemical and physiological parameters will influence transcorneal permeability.

In the current study we prepared the melt cast films with 10 % w/w and 20 % w/w HT loads such that the total amount of HT per unit dosage of 4 mm \times 2 mm film was maintained at 0.8 mg and 1.6 mg, respectively. The thickness of the films was maintained between 0.2 mm - 0.4 mm. PEO N10 was selected as the matrix forming material because of its good aqueous

solubility, low viscosity and low toxicity [39]. Since the polymer is water soluble, it can easily transform into a gel and be slowly washed away by the tear fluid. PEO N10 has a low melting point and an excellent film forming ability. This property helps in achieving smooth flexible films at low temperatures and can thus be employed to develop matrix films for thermo-sensitive compounds. Surface of the film was flat and smooth avoiding any discomfort *in vivo*. Uniform distribution of HT was achieved within the polymeric matrix by continuous geometric dilution as confirmed by both FTIR and HPLC analysis. PEO N10 has been reported to form simple binary eutectic mixtures due to its low entropy of fusion thereby improving drug release from the matrix [40, 41]. Endothermic peak shifts observed in the DSC thermograms could be because of this eutectic mixture formation.

Side-by-side diffusion apparatus was employed to determine flux across the cornea. A modified protocol was used to represent periocular loss of HT from the film. To the best of our knowledge, this is the first time an *in vitro* model has been used to study transcorneal permeation in the presence of precorneal/periocular loss. In this study, flux across the Spectra/Por® membrane, used on the precorneal side, was 1.7-fold greater than the corneal tissue. The ratio of precorneal loss to corneal penetration was thus 1.7:1 under the conditions tested. By changing the experimental parameters (e.g. use of different backing membranes, vertical apparatus, sandwiched cassettes, continuous dilution of the donor chamber solution) periocular/precorneal loss can be increased to mimic precorneal loss *in vivo* and to develop *in vitro in vivo correlations*. The apparatus/set-up can be easily modified to accommodate various types of ophthalmic formulations.

Release of HT from the film, with or without sieve, followed the Higuchi model with coefficient of determination (R^2) 0.9899 and 0.9873, respectively. The results demonstrate that the sieve did not act as a barrier to HT release and diffusion in the release medium. Flux across the membranes exhibited zero-order kinetics. *In vitro* transcorneal flux was several folds greater than that obtained with other formulations reported in the literature [36], even in the presence of a precorneal loss. This demonstrates the value of the melt-cast topical HT dosage form.

The whole eye globes obtained from Pel-Freez Biologicals served as a good *ex vivo* model. HT film required approximately 30 min to transform into a gel in the absence of any tear fluid. The concentrations observed in the RC were 3-fold higher when compared to the levels in the AH and VH. The results suggest that the film was preferentially delivering HT to the posterior segment of eye through conjunctival-scleral pathway. Considering the data, from the subsequent *in vivo* studies, ocular tissue concentrations of HT in AH, VH and RPE were found to be overestimated in the *ex vivo* model due to lack of vascular and lymphatic drainage systems.

As expected, and unlike the *ex vivo* studies, HT films transformed into a gel in less than 5 min following topical application. This was much quicker when compared to the *ex vivo* study due to the presence of tear fluids. Allergic reactions such as inflammation or redness or excessive tearing were not observed throughout the duration of the study. Results from the topical HT films indicate that significant levels of HT can be delivered to the posterior segment of the eye with these matrix film formulations. With the 10 %w/w HT film

significant amounts of HT was detected in both VH and RC (Table I). On doubling the amount of HT in the matrix, VH and RC levels markedly increased by 28- and 3-folds, respectively. Thus, a dose dependent concentration profile was observed from the matrix system. Significant HT levels were detected in the cornea, sclera, IC and AH 1 h post topical application of the matrix. The concentration profile, higher HT concentrations in the RC when compared to the VH, was consistent with scleral absorption pathway, as also suggested by the *ex vivo* studies. High drug concentration in the PEO matrix in close contact with the ocular tissues could favor direct partitioning from the matrix into the ocular tissues. This might be one of the possible reasons for achieving significant intraocular tissue concentrations from the matrix film.

Ramesh *et al.*, have previously evaluated ocular bioavailability of HT through intravenous and topical routes of application [42]. In these studies, 1 %w/v HT solution (Dose: 1 mg) for topical instillation was prepared using 10 %w/v HP β CD and 10 %w/v RM β CD. HT concentrations in the AH, VH, RC and IC achieved with the 1 %w/v HT-CD solution (dose: 1 mg; 100 μ L instilled volume) were approximately 3-5 folds lower than the levels obtained with the 10 %w/w HT film (Dose: 0.8 mg) in the current study. Concentrations in the sclera and cornea were similar in both the cases. When benzalkonium chloride (BAK) was included in the HT-CD solution formulation [42], the ocular tissue concentrations achieved were 2-fold higher than that obtained with the 10 %w/w film, which did not contain any BAK, at the 1 h time point [42]. The 20 %w/w HT film, however, was able to deliver significantly higher HT levels in all cases. Thus, although the melt-cast film did not have any preservatives or solubilizers, the intraocular tissue concentrations achieved with this dosage form were very high.

HT is rapidly eliminated from the ocular tissues due to choroidal and lymphatic drainage. HT levels in all ocular tissues declined rapidly after application of both 10 % and 20 %w/w film (Figure VIIIA & B). Less than 50% of the concentration determined at the 1 h time point remained in the VH, RC and IC 3 h post topical application, suggesting a vitreal half-life of less than 2 h. The results are consistent with vitreal half-life of 110 minutes reported in earlier studies [42]. Matrix films containing 20% HT, however, maintained significant levels in all the ocular tissues at the end of 3 h. In fact, with the 20 %w/v HT films a significant amount of HT was maintained in the VH and RC and other ocular tissues, even after 6 h post application.

Smith *et al.* reported that at 0.1-0.3 μ M (30.2 - 90.7 ng/mL) concentrations, HT demonstrates neuroprotective activity when mouse primary cortical neurons were subjected to a pro-apoptotic insult by exposing them to staurosporine [43]. All studies determining IC₅₀ values report solution concentrations and not actual tissue concentrations. Thus, the AH and VH concentrations, which are in equilibrium with the anterior and posterior segment ocular tissues, serve as good therapeutic response indicators for IC and RC sites. Considering that the VH is on the receiving side with the scleral side being the dosing side (topical application) it can be expected that the HT concentrations in the RC or IC will be well within the therapeutic range at least for as long as the VH and AH concentrations are within the IC₅₀ range. In the current study we observe that even at the 6h time point, the levels of HT in VH (30 ng/mL), are within this range. Although the AH was not analyzed at

the 6h time point, since the AH concentrations were typically several folds greater than the VH concentrations at all time-points, following topical application, it can be concluded that the AH concentrations would also be within the neuroprotective concentration range at the 6h time point. Thus, with the 20% matrix films, ocular tissue HT concentrations were maintained within and above levels required for neuroprotectant activity for at least 6h post topical application.

With respect to anti-oxidant activity, HT levels at the end of 1 h in the AH (4.2 µg/mL) was greater than the IC₅₀ values for peroxy-nitrites (IC₅₀: 4.67 µM; 1.4 µg/mL) and superoxide inhibition (IC₅₀: 7.47 µM; 2.3 µg/mL) [13]. With the 20 %w/w film, at the end of 1h, HT levels in both AH and VH were above these IC₅₀ values. Levels of HT in AH (3.4 µg/mL) were maintained above the IC₅₀ values for peroxy-nitrites and superoxide inhibition even at the end of 3h, following topical application of the 20 %w/w film.

In terms of anti-inflammatory activity, Yang et al. reported that at 1-10 µM (0.3 – 3.02 µg/mL) HT concentrations, cellular levels of COX-2 and PEG2 are markedly attenuated [44]. With both the 10% and 20 %w/w films, HT levels in the AH (1.2 and 3.4 µg/mL, respectively) were maintained within the concentration range required for COX-2 and PEG2 inhibition, even at the end of 3h.

Thus, the polymeric matrix film was successfully able to deliver and maintain levels of HT required for neuroprotectant, anti-oxidant and anti-inflammatory activity in the ocular tissues. As mentioned earlier, the AH and VH concentrations represent the innermost ocular tissues (receiver solutions) in the anterior and posterior segments, respectively, for a topical route of application. Thus, the concentrations in the retina, choroid, cornea or iris-ciliary bodies would be significantly higher compared to what would be achieved if the AH or VH concentrations were to represent donor concentrations (e.g. intravitreal injection).

5. Conclusion

In conclusion, appreciable ocular tissue concentrations were achieved using non-invasive topical melt-cast films. A 2-fold increase in HT content in the matrix film led to several fold increase in the HT concentration in the ocular tissues. With the 20 %w/w HT film high concentrations of HT were maintained in the posterior segment ocular tissues even at 3 h post topical application. Quantifiable levels of HT was still retained in the VH and RC even after 6 h. Corneal histology studies indicate that the formulations did not produce any damage to the ocular tissues. Thus, the melt-cast matrix films appear to be a promising approach for drug delivery to the back-of-the-eye.

Acknowledgments

This work was supported by National Institute of General Medical Sciences, National Institutes of Health (Grant P20GM104932) and SBAHQ-10-I-0309. The content is solely the responsibility of the authors and does not necessarily represent the official views of the National Institutes of Health.

References

1. Arden GB. The absence of diabetic retinopathy in patients with retinitis pigmentosa: implications for pathophysiology and possible treatment. *Br J Ophthalmol.* 2001; 85:366–370. [PubMed: 11222350]
2. Kowluru RA, Odenbach S. Role of interleukin-1beta in the development of retinopathy in rats: effect of antioxidants. *Invest Ophthalmol Vis Sci.* 2004; 45:4161–4166. [PubMed: 15505070]
3. Bressler NM, Bressler SB, Fine SL. Age-related macular degeneration. *Surv Ophthalmol.* 1988; 32:375–413. [PubMed: 2457955]
4. Wilkinson-Berka JL. Vasoactive factors and diabetic retinopathy: vascular endothelial growth factor, cyclooxygenase-2 and nitric oxide. *Curr Pharm Des.* 2004; 10:3331–3348. [PubMed: 15544519]
5. Watkins PJ. Diabetic complications: retinopathy. *Br Med J (Clin Res Ed).* 1982; 285:425–427.
6. Fong DS, Aiello L, Gardner TW, King GL, Blankenship G, Cavallerano JD, Ferris FL 3rd, Klein R. Diabetic retinopathy. *Diabetes Care.* 2003; 26:226–229. [PubMed: 12502685]
7. Aizu Y, Oyanagi K, Hu J, Nakagawa H. Degeneration of retinal neuronal processes and pigment epithelium in the early stage of the streptozotocin-diabetic rats. *Neuropathology.* 2002; 22:161–170. [PubMed: 12416555]
8. Young RW. Pathophysiology of age-related macular degeneration. *Surv Ophthalmol.* 1987; 31:291–306. [PubMed: 3299827]
9. Hingorani T, Gul W, Elshohly M, Repka MA, Majumdar S. Effect of ion pairing on in vitro transcorneal permeability of a Delta(9) -tetrahydrocannabinol prodrug: potential in glaucoma therapy. *J Pharm Sci.* 2012; 101:616–626. [PubMed: 21989812]
10. R S, Adelli Goutham R, Majumdar Soumyajit. Phytochemicals in ocular health: Therapeutic potential and delivery challenges. *World J Pharmacol.* 2013; 2:18–34.
11. Choi EJ. Antioxidative effects of hesperetin against 7,12-dimethylbenz(a)anthracene-induced oxidative stress in mice. *Life Sci.* 2008; 82:1059–1064. [PubMed: 18433790]
12. Hwang SL, Yen GC. Neuroprotective effects of the citrus flavanones against H₂O₂-induced cytotoxicity in PC12 cells. *J Agric Food Chem.* 2008; 56:859–864. [PubMed: 18189359]
13. Kim JY, Jung KJ, Choi JS, Chung HY. Hesperetin: a potent antioxidant against peroxynitrite. *Free Radic Res.* 2004; 38:761–769. [PubMed: 15453641]
14. Miyake Y, Minato K, Fukumoto S, Yamamoto K, Oya-Ito T, Kawakishi S, Osawa T. New potent antioxidative hydroxyflavanones produced with *Aspergillus saitoi* from flavanone glycoside in citrus fruit. *Biosci Biotechnol Biochem.* 2003; 67:1443–1450. [PubMed: 12913285]
15. Jung HA, Jung MJ, Kim JY, Chung HY, Choi JS. Inhibitory activity of flavonoids from *Prunus davidiana* and other flavonoids on total ROS and hydroxyl radical generation. *Arch Pharm Res.* 2003; 26:809–815. [PubMed: 14609128]
16. Pollard SE, Whiteman M, Spencer JP. Modulation of peroxynitrite-induced fibroblast injury by hesperetin: a role for intracellular scavenging and modulation of ERK signalling. *Biochem Biophys Res Commun.* 2006; 347:916–923. [PubMed: 16857166]
17. Hirata A, Murakami Y, Shoji M, Kadoma Y, Fujisawa S. Kinetics of radical-scavenging activity of hesperetin and hesperidin and their inhibitory activity on COX-2 expression. *Anticancer Res.* 2005; 25:3367–3374. [PubMed: 16101151]
18. Olszanecki R, Gebaska A, Kozlovski VI, Gryglewski RJ. Flavonoids and nitric oxide synthase. *J Physiol Pharmacol.* 2002; 53:571–584. [PubMed: 12512693]
19. Dansky KH, Yant B, Jenkins D, Dellasega C. Qualitative analysis of telehomecare nursing activities. *J Nurs Adm.* 2003; 33:372–375. [PubMed: 12909786]
20. Chiou GC, Xu XR. Effects of some natural flavonoids on retinal function recovery after ischemic insult in the rat. *J Ocul Pharmacol Ther.* 2004; 20:107–113. [PubMed: 15117566]
21. Ameer B, Weintraub RA, Johnson JV, Yost RA, Rouseff RL. Flavanone absorption after naringin, hesperidin, and citrus administration. *Clin Pharmacol Ther.* 1996; 60:34–40. [PubMed: 8689809]

22. Srirangam R, Hippalgaonkar K, Avula B, Khan IA, Majumdar S. Evaluation of the intravenous and topical routes for ocular delivery of hesperidin and hesperetin. *J Ocul Pharmacol Ther.* 28:618–627. [PubMed: 22794525]
23. Yanez JA, Remsberg CM, Miranda ND, Vega-Villa KR, Andrews PK, Davies NM. Pharmacokinetics of selected chiral flavonoids: hesperetin, naringenin and eriodictyol in rats and their content in fruit juices. *Biopharm Drug Dispos.* 2008; 29:63–82. [PubMed: 18058792]
24. Srirangam R, Hippalgaonkar K, Majumdar S. Intravitreal kinetics of hesperidin, hesperetin, and hesperidin G: effect of dose and physicochemical properties. *J Pharm Sci.* 101:1631–1638. [PubMed: 22228207]
25. Loftssona T, Jarvinen T. Cyclodextrins in ophthalmic drug delivery. *Adv Drug Deliv Rev.* 1999; 36:59–79. [PubMed: 10837709]
26. Geroski DH, Edelhauser HF. Drug delivery for posterior segment eye disease. *Invest Ophthalmol Vis Sci.* 2000; 41:961–964. [PubMed: 10752928]
27. Wu Y, Yao J, Zhou J, Dahmani FZ. Enhanced and sustained topical ocular delivery of cyclosporine A in thermosensitive hyaluronic acid-based in situ forming microgels. *Int J Nanomedicine.* 2013; 8:3587–3601. [PubMed: 24092975]
28. Fathi M, Varshosaz J, Mohebbi M, Shahidi F. Hesperetin-Loaded Solid Lipid Nanoparticles and Nanostructure Lipid Carriers for Food Fortification: Preparation, Characterization, and Modeling. *Food Bioprocess Technol.* 2013
29. Ficarra R, Tommasini S, Raneri D, Calabro ML, Di Bella MR, Rustichelli C, Gamberini MC, Ficarra P. Study of flavonoids/beta-cyclodextrins inclusion complexes by NMR, FT-IR, DSC, X-ray investigation. *J Pharm Biomed Anal.* 2002; 29:1005–1014. [PubMed: 12110385]
30. Gaudana R, Ananthula HK, Parenky A, Mitra AK. Ocular drug delivery. *AAPS J.* 2010; 12:348–360. [PubMed: 20437123]
31. Maiti K, Mukherjee K, Murugan V, Saha BP, Mukherjee PK. Exploring the effect of Hesperetin-HSPC complex--a novel drug delivery system on the in vitro release, therapeutic efficacy and pharmacokinetics. *AAPS PharmSciTech.* 2009; 10:943–950. [PubMed: 19629709]
32. Majumdar S, Hingorani T, Srirangam R, Gadepalli RS, Rimoldi JM, Repka MA. Transcorneal permeation of L- and D-aspartate ester prodrugs of acyclovir: delineation of passive diffusion versus transporter involvement. *Pharm Res.* 2009; 26:1261–1269. [PubMed: 18839288]
33. M, Fathi; Varshosaz, J.; Mohebbi, M.; Shahidi, F. Hesperetin-Loaded Solid Lipid Nanoparticles and Nanostructure Lipid Carriers for Food Fortification: Preparation, Characterization, and Modeling. *Food Bioprocess Technol.* 2012
34. Becker U, Ehrhardt C, Schneider M, Muys L, Gross D, Eschmann K, Schaefer UF, Lehr CM. A comparative evaluation of corneal epithelial cell cultures for assessing ocular permeability. *Altern Lab Anim.* 2008; 36:33–44. [PubMed: 18333713]
35. Majumdar S, Srirangam R. Solubility, stability, physicochemical characteristics and in vitro ocular tissue permeability of hesperidin: a natural bioflavonoid. *Pharm Res.* 2009; 26:1217–1225. [PubMed: 18810327]
36. Srirangam R, Majumdar S. Passive asymmetric transport of hesperetin across isolated rabbit cornea. *Int J Pharm.* 394:60–67. [PubMed: 20438820]
37. Abelson MB, Udell IJ, Weston JH. Normal human tear pH by direct measurement. *Arch Ophthalmol.* 1981; 99:301. [PubMed: 7469869]
38. Norm MS. Tear fluid pH in normals, contact lens wearers, and pathological cases. *Acta Ophthalmol (Copenh).* 1988; 66:485–489. [PubMed: 3218470]
39. Fruijtier-Polloth C. Safety assessment on polyethylene glycols (PEGs) and their derivatives as used in cosmetic products. *Toxicology.* 2005; 214:1–38. [PubMed: 16011869]
40. Law D, Wang W, Schmitt EA, Qiu Y, Krill SL, Fort JJ. Properties of rapidly dissolving eutectic mixtures of poly(ethylene glycol) and fenofibrate: the eutectic microstructure. *J Pharm Sci.* 2003; 92:505–515. [PubMed: 12587112]
41. Craig DQ. The mechanisms of drug release from solid dispersions in water-soluble polymers. *Int J Pharm.* 2002; 231:131–144. [PubMed: 11755266]

42. Srirangam R, Hippalgaonkar K, Avula B, Khan IA, Majumdar S. Evaluation of the intravenous and topical routes for ocular delivery of hesperidin and hesperetin. *J Ocul Pharmacol Ther.* 2012; 28:618–627. [PubMed: 22794525]
43. Rainey-Smith S, Schroetke LW, Bahia P, Fahmi A, Skilton R, Spencer JP, Rice-Evans C, Rattray M, Williams RJ. Neuroprotective effects of hesperetin in mouse primary neurones are independent of CREB activation. *Neurosci Lett.* 2008; 438:29–33. [PubMed: 18467030]
44. Yang HL, Chen SC, Senthil Kumar KJ, Yu KN, Lee Chao PD, Tsai SY, Hou YC, Hseu YC. Antioxidant and anti-inflammatory potential of hesperetin metabolites obtained from hesperetin-administered rat serum: an ex vivo approach. *J Agric Food Chem.* 60:522–532. [PubMed: 22098419]

Abbreviations

| | |
|------------------------|--|
| HD | Hesperidin |
| HT | Hesperetin |
| PEO N10 | polyethylene oxide N10 |
| DR | diabetic retinopathy |
| AMD | age related macular degeneration |
| DME | diabetic macular edema |
| PVR | proliferative vitreo-retinopathy |
| CNV | choroidal neovascularization |
| WHO | World Health Organization |
| RPE | retinal pigmented epithelium |
| ROS | reactive oxidative species |
| ERKs | extracellular-signal-regulated kinases |
| COX | cyclooxygenase |
| PGE₂ | prostaglandin E ₂ |
| IPBS | isotonic phosphate buffered saline |
| HBSS | Hank's balanced salt solution |
| DSC | differential scanning calorimetry |
| FTIR | Fourier transform infrared spectroscopy |
| ATR | attenuated total reflectance |
| HPLC-UV | High performance liquid chromatography- Ultra violet |
| mM | millimolar |
| µg | microgram |
| DMSO | dimethyl sulfoxide |
| ACN | acetonitrile |
| AH | aqueous humor |

| | |
|-----------|---------------------|
| VH | vitreous humor |
| IC | iris ciliary bodies |
| RC | retina-choroid |

Author Manuscript

Author Manuscript

Author Manuscript

Author Manuscript

Highlights

- Melt-cast film for efficient delivery of hesperetin (HT) to the back-of-the eye.
- Release of HT from the film followed the Higuchi model.
- Development of “membrane-film-cornea” sandwich model to mimic precorneal loss.
- Matrix film delivers neuroprotectant levels of HT for at least 6h post application.

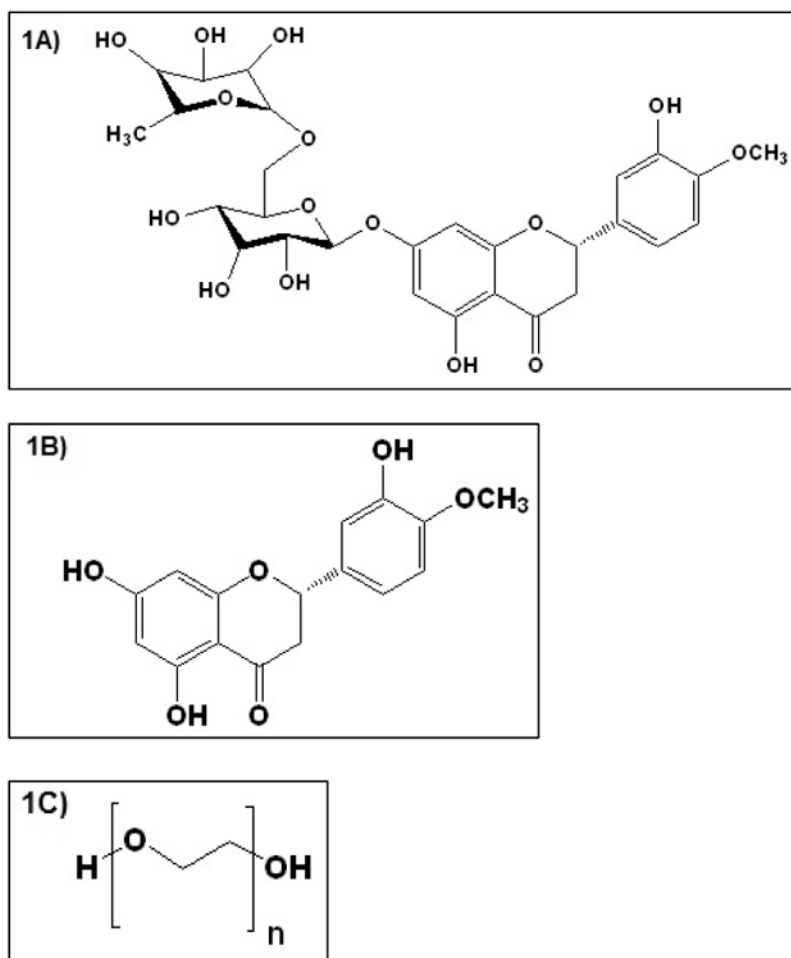


Figure I.
Chemical structure of A) Hesperidin, B) Hesperetin and C) PEO N10 respectively.

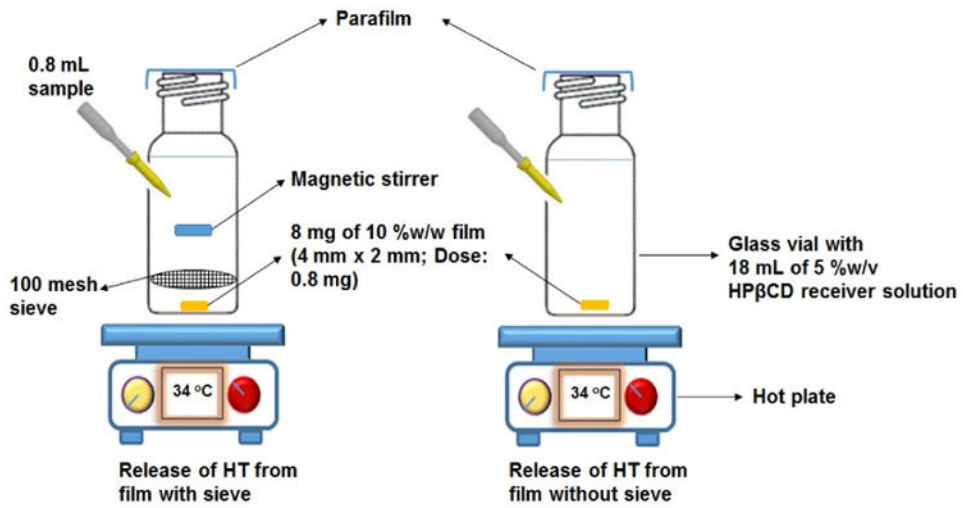


Figure II.
Release of HT from film using standard US 100 mesh sieve and without sieve.

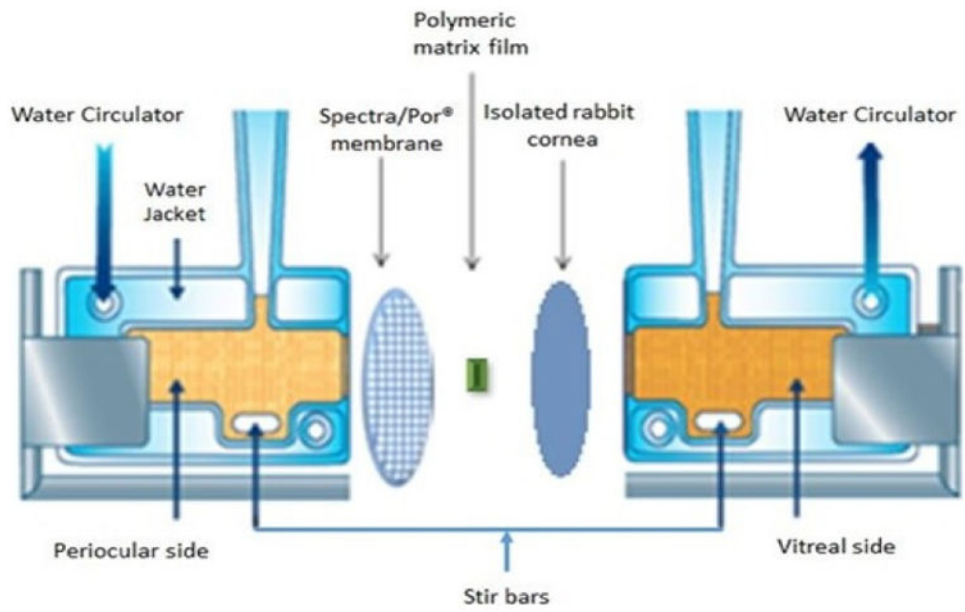


Figure III. Side-by-side diffusion apparatus setup used for *in vitro* release and transcorneal permeability studies.

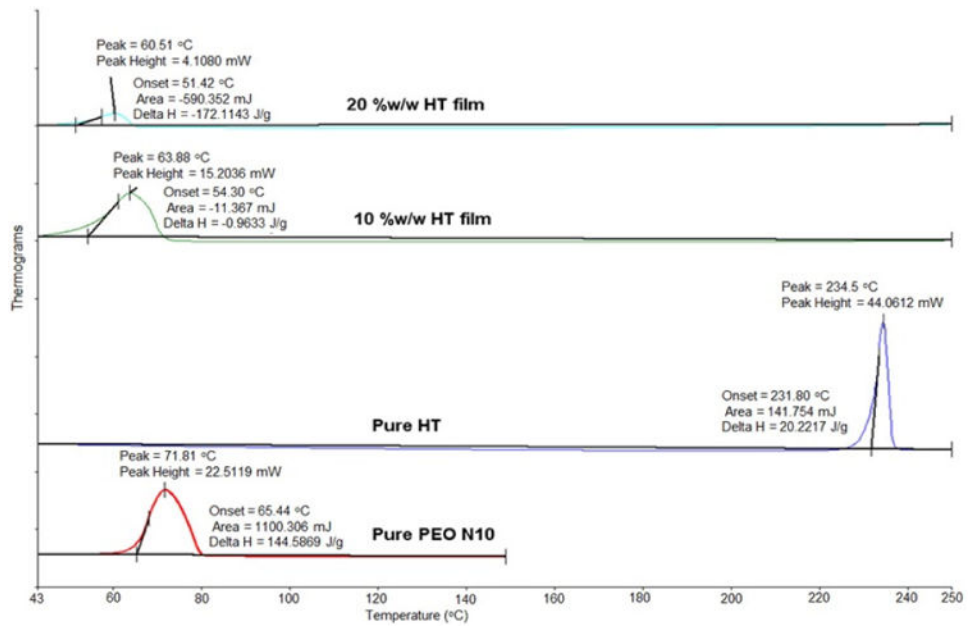


Figure IV. Differential scanning calorimetry thermograms of hesperetin (HT) polymeric matrix film, pure PEO N10 and pure HT.

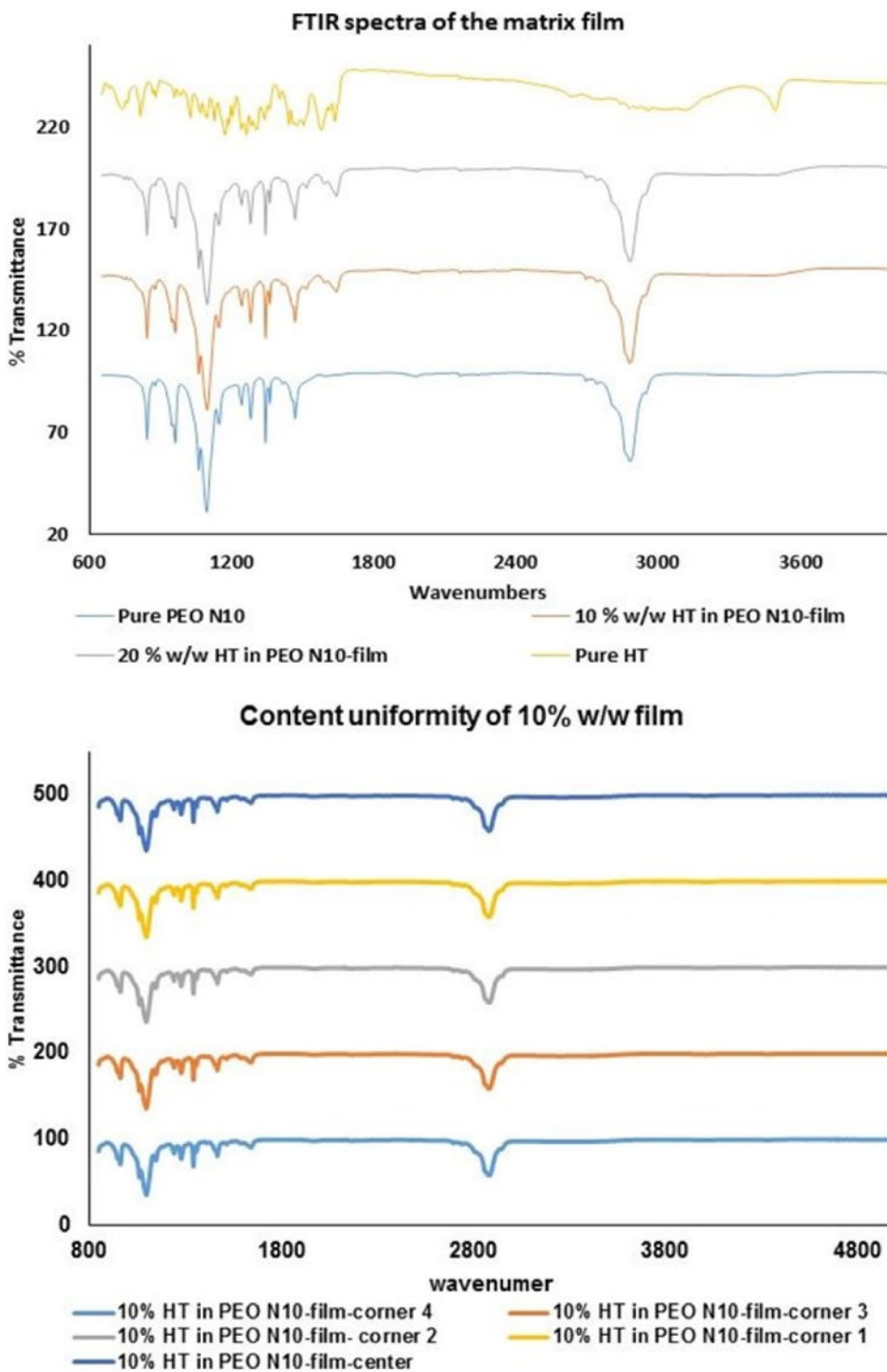


Figure V.

A. FTIR spectral images of pure PEO N10, pure hesperetin (HT), 10 %w/w hesperetin polymeric matrix film and 20 %w/w hesperetin polymeric matrix film.

B. FTIR spectral images of hesperetin (HT) at randomly selected areas on 13mm circular polymeric matrix film.

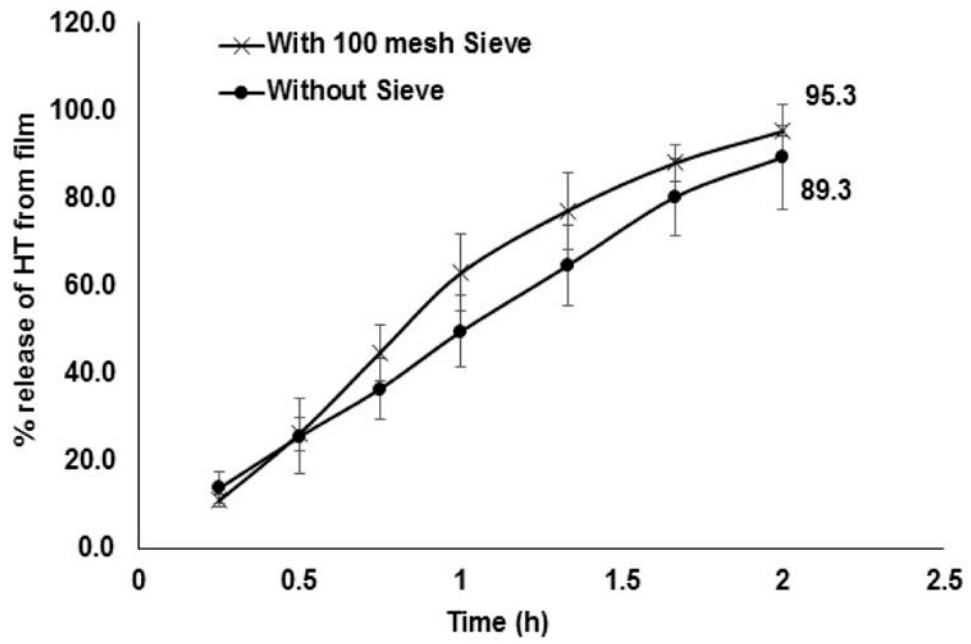


Figure VI.
Percentage release of HT from 10 % w/w film across the standard US 100 mesh and without sieve.

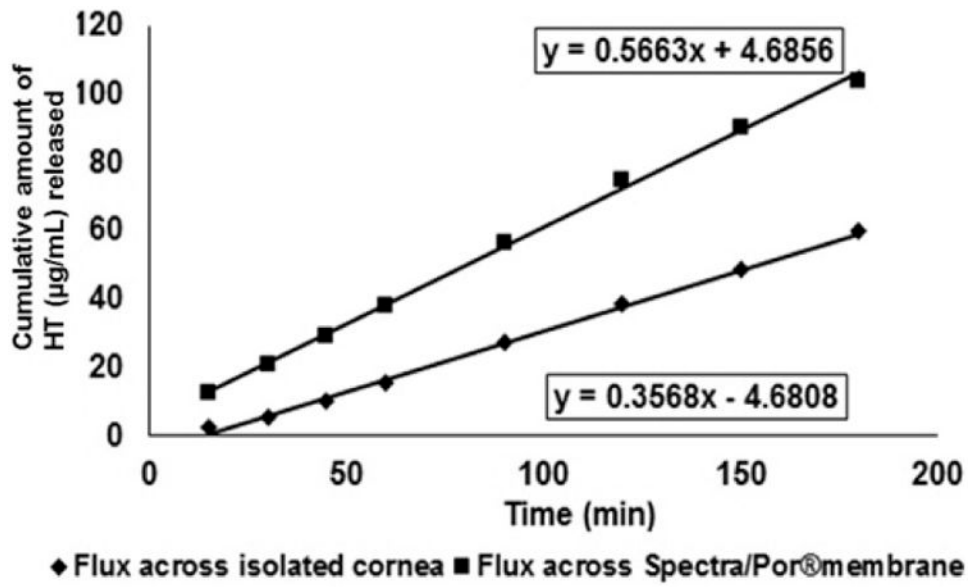


Figure VII.

In vitro transcorneal permeability of hesperetin (HT) from 10 %w/w matrix film across isolated rabbit cornea.

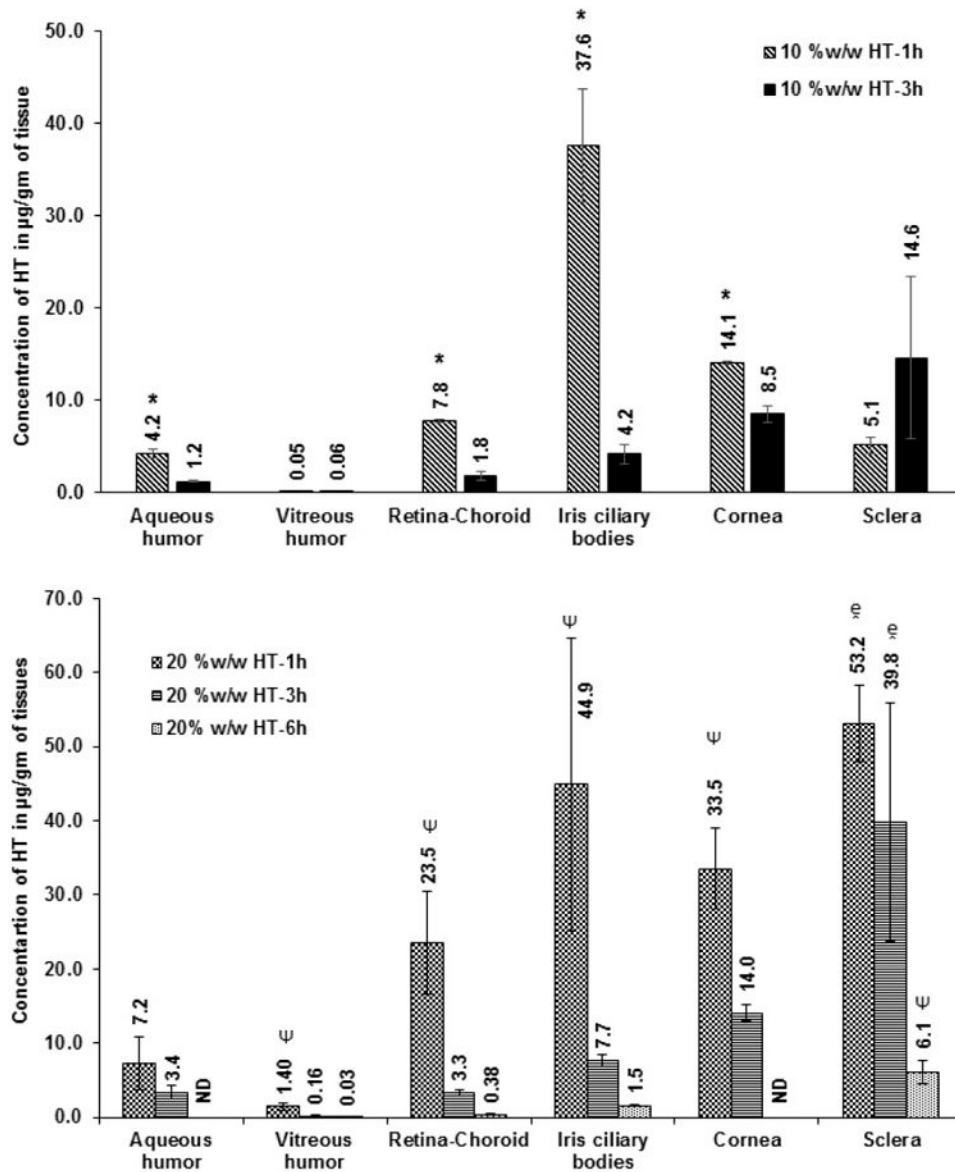


Figure VIII.

A. Ocular tissue hesperetin (HT) concentrations ($\mu\text{g/gm}$ of tissue) obtained from 10 %w/w films, 1 h and 3 h post application. All experiments were performed in triplicate. AH: Aqueous Humor; VH: Vitreous Humor; RC: Retina-Choroid; IC: Iris-Ciliary. ND - not determined. *- Significantly different from 10 %w/w HT-3h.

B. Ocular tissue hesperetin (HT) concentrations ($\mu\text{g/gm}$ of tissue) obtained from 20 %w/w film 1 h, 3 h or 6 h post topical application. All experiments were performed in triplicate. AH- Aqueous Humor; VH- Vitreous Humor; RC- Retina-Choroid & IC-Iris-Ciliary. ND- Not determined. - Significantly different from 20% w/w HT film-6h and Ψ -Significantly different from 20 %w/w HT 1h & 20 %w/w HT 3h.

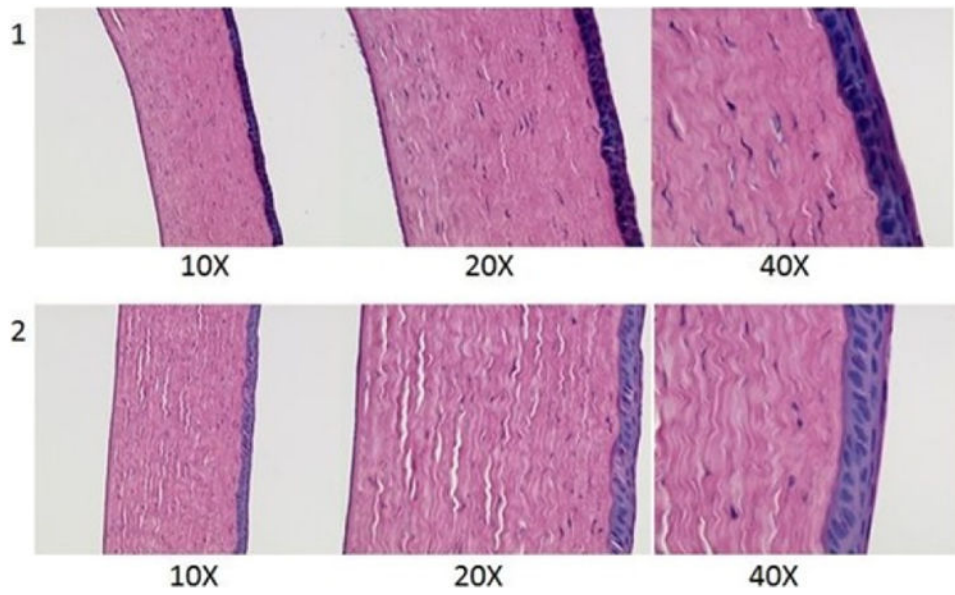


Figure IX.
Histological images of rabbit corneas exposed to 1) IPBS & 2) 20 % w/w hesperetin film for 6h.

Ocular tissue hesperetin (HT) concentrations ($\mu\text{g}/\text{gm}$ of tissue) obtained from 10 % w/w & 20 % w/w films 1, 3 or 6 hours post topical application. All experiments were performed in triplicate.

Table I

| Formulation | Dose (mg) | Duration (h) | $\mu\text{g}/\text{gm}$ of Tissue | | | | | |
|-----------------|-----------|--------------|-----------------------------------|-----------------|-----------------|-----------------|----------------|-----------------|
| | | | AH | VH | RC | IC | Cornea | Sclera |
| 10% w/w HT film | 0.8 mg | 1h | 4.2 \pm 0.4 | 0.05 \pm 0.03 | 7.8 \pm 0.2 | 37.6 \pm 6.2 | 14.1 \pm 0.2 | 5.1 \pm 0.9 |
| 10% w/w HT film | 0.8 mg | 3h | 1.2 \pm 0.1 | 0.06 \pm 0.02 | 1.8 \pm 0.5 | 4.2 \pm 1.1 | 8.5 \pm 0.9 | 14.6 \pm 8.8 |
| 20% w/w HT film | 1.6 mg | 1h | 7.2 \pm 3.6 | 1.4 \pm 0.5 | 23.5 \pm 6.9 | 44.9 \pm 19.7 | 33.5 \pm 5.4 | 53.2 \pm 5.2 |
| 20% w/w HT film | 1.6 mg | 3h | 3.4 \pm 0.9 | 0.16 \pm 0.07 | 3.3 \pm 0.4 | 7.7 \pm 0.8 | 14.1 \pm 1.1 | 39.8 \pm 16.1 |
| 20% w/w HT film | 1.6 mg | 6h | ND | 0.03 \pm 0.02 | 0.38 \pm 0.02 | 1.5 \pm 0.1 | ND | 6.1 \pm 1.6 |

AH - Aqueous Humor; VH - Vitreous Humor; RC - Retina-Choroid & IC - Iris Ciliary bodies.